Topology Optimization Integrated Deep Learning for Multiphysics Problems

Hesaneh Kazemi [*]
University of California San Diego, San Diego, CA, 92093

Carolyn C. Seepersad [†]
University of Texas Austin, Austin, TX, 78712

H. Alicia Kim[‡]
University of California San Diego, San Diego, CA, 92093

This work presents a method for generating concept designs for coupled multiphysics problems by employing Generative Adversarial Networks (GANs). Since the optimal designs of multiphysics problems often contain a combination of features that can be found in the single-physics solutions, we investigate the feasibility of learning the optimal design from the single-physics solutions, in order to produce concept designs for problems that are governed by a combination of these single-physics. We employ GANs in order to produce optimal topologies similar to the results of level set topology optimization (LSTO) by finding a mapping between the sensitivity fields of specific boundary conditions, and the optimal topologies. To find this mapping, we perform image-to-image translation GAN training with a combination of structural, heat conduction, and a relatively smaller number of coupled structural and heat conduction data. We observe that the predicted topologies using GAN for coupled multiphysics problems are very similar to those generated by level set topology optimization, which can then be used as the concept designs for further detailed design. We show that using a combination of multiple single-physics data in the training improves the prediction of GAN for multiphysics problems. We provide several examples to demonstrate this.

I. Nomenclature

$f(x)$	=	objective function
$g(x)$	=	constraint function
$\mathbf{U}$	=	displacement vector
$\mathbf{F}$	=	force vector
$\mathbf{K}$	=	mechanical stiffness matrix
$\mathbf{T}$	=	temperature field
$\mathbf{Q_t}$	=	heat flux
$\mathbf{K_t}$	=	thermal stiffness matrix
$V_f(x)$	=	volume fraction
V_f^*	=	volume fraction limit
$\mathbf{F_t}$	=	thermal load vector
$\mathbf{F_m}$	=	mechanical load vector
w_m	=	weight for mechanical objective
w_t	=	weight for thermal objective
$\phi(x)$	=	level set fucntion
Ω	=	structural domain
Γ	=	boundary
V_n	=	normal velocity

[*]postdoctoral scholar, Structural Engineering Department, 9500 Gilman Drive, Mail Code 0085, San Diego CA 92093
[†]Professor, Department of Mechaninal Engineering, 204 E. Dean Keeton Street ETC II 5.160. Austin, Texas 78712
[‡]Professor, Structural Engineering Department, 9500 Gilman Drive, Mail Code 0085, San Diego CA 92093 Associate fellow

k	=	iteration number
r	=	a discrete node in the design domain
V_{nr}	=	the normal velocity at node r
t	=	fictitious time domain
s_f	=	shape sensitivity for the objective function
s_{gm}	=	shape sensitivity for the constraint function
$\mathbf{d}$	=	search direction for the boundary update
α	=	the distance travelled along the search direction
$\mathcal{L}_{GAN}$	=	loss function
$\mathcal{L}_{cGAN}$	=	loss function
$\mathcal{L}_{L1}$	=	loss function
G	=	generator
D	=	discriminator

II. Introduction

Topology optimization can generate novel designs by finding the optimal distribution of material in a design space. Existing methods include density-based approaches [1–4], geometry projection methods [5–9], and level set approaches [10–14]. These methods have been extensively applied over the past few decades for various objectives and physics, such as design of structures for the best performance, or of microstructures for desired material properties.

With advances in data driven approaches, deep learning algorithms have been employed in topology optimization to design for minimum compliance [15–21] or thermal compliance [22–24]. One promise of using deep learning algorithms in topology optimization is to reduce the computational cost. Nevertheless, using topology optimization to solve a single-physics problem, such as linear elasticity, is usually straightforward and does not require significant computational resources. Considering the computational cost required for generating data and training, it is difficult to justify the advantage of using deep learning algorithms for such problems solely for the purpose of increasing the computational efficiency.

In complex problems, however, given the importance of considering coupled multiphysics in multifunctional structures, topology optimization can be substantially more challenging. To the best of our knowledge, deep learning has not been applied to topology optimization of coupled multiphysics problems. In this work, we explore using single-physics data generated for different physics for training, which are generally easier to obtain, with the aim to find the optimal topology for a problem that accounts for the combination of multiple physics.

Deep learning algorithms have also been employed to learn complex mappings between problem input variables and optimal topologies. In [25] a new data-driven design representation is proposed that uses an augmented variational autoencoder to generate topologies from a low-dimensional latent space. In [26] a deep generative design framework is proposed, which generates several design options that are optimized for engineering performance. In [18], a deep learning-based method is presented to find a mapping between a given boundary condition and the optimized structure. A convolutional neural network based encoder and decoder network is trained using the low resolution training dataset, and is followed by a two-stage refinement. In [27], the use of conditional generative adversarial networks (cGANs) is explored to aid concept generation, by generating a compact latent representation of structures designed by topology optimization. In [20], a mapping between various physical response fields computed over the initial domain and the optimal topologies is found.

We employ image-to-image translation GAN algorithms to generate concept designs for coupled multiphysics problems. We adapt the idea of [20] where physical fields computed over the initial domain are used as input images. As opposed to [20], we only use the strain energy density field. For training, we use a combination of two single-physics response fields, i.e. structural and heat conduction sensitivity, as well as a relatively smaller number of coupled multiphysics data. We investigate the effect of the number of multiphysics data on the accuracy of the results. We compare these results with those that have been trained with multiphyscis data only.

The structure of the paper is as follows: In Section III we briefly describe the topology optimization formulation for structural, heat conduction and coupled problems and the level set topology optimization method that we use to generate the training data. Section IV discusses the GAN algorithm [28] and the conditional GAN method for image-to-image translation that we employ in this work. In Section V we describe our methodology. Section VI presents the numerical results, from which the conclusions are drawn in Section VII.

III. Topology Optimization

The topology optimization problem in the general form can be written as

$$\underset{x}{\textbf{minimize}}\, f(x)$$

$$\textbf{subject to} \quad g(x) \le g^* \tag{1}$$

In this work, we consider three types of problems: structural problems, heat conduction problems, and coupled structural and heat conduction problems.

A. Structural Problem Formulation

For structural problems, the optimization problem is formulated to minimize structural compliance subject to a volume (area) fraction constraint:

$$\underset{x}{\textbf{minimize}}\, f(x) = \mathbf{U}^T \mathbf{K} \mathbf{U}$$

$$\textbf{subject to} \quad V_f(x) \le V_f^* \tag{2}$$
$$\mathbf{K}\mathbf{U} = \mathbf{F},$$

where $\mathbf{U}$ and $\mathbf{F}$ are the global displacement and force vectors, respectively, $\mathbf{K}$ is the global stiffness matrix, $V_f(x)$ is the design volume fraction and V_f^* is the prescribed volume fraction.

B. Heat Conduction Problem Formulation

For heat conduction problems, the optimization problem is

$$\underset{x}{\textbf{minimize}}\, f(x) = \mathbf{T}^T \mathbf{K_t} \mathbf{T}$$

$$\textbf{subject to} \quad V_f(x) \le V_f^* \tag{3}$$
$$\mathbf{K_t}\mathbf{T} = \mathbf{Q_t}$$

where $\mathbf{T}$ is the temperature field, $\mathbf{K_t}$ is the thermal stiffness matrix and $\mathbf{Q_t}$ is the heat flux. Similar to the structural problem formulation, a volume fraction constraint is imposed.

C. Coupled Multiphysics Problem Formulation

The third type of problem that we consider in this work is weakly-coupled thermoelastic problems, where the temperature distribution causes the structure to expand or contract, resulting in thermal strain. Finite element analysis of this problem reduces to solving two linear systems of equations [29]. First, the thermal problem is solved to compute the temperature field:

$$\mathbf{K_t}\mathbf{T} = \mathbf{Q_t}. \tag{4}$$

Then, the thermoelastic force $\mathbf{F_t}$ resulting from this temperature field is added to the mechanical force $\mathbf{F_m}$, and the following equation is solved to compute the displacement under mechanical and thermal loads:

$$\mathbf{K}\mathbf{U} = \mathbf{F_m} + \mathbf{F_t}. \tag{5}$$

The optimization problem can then be written as

$$\underset{x}{\textbf{minimize}}\, f(x) = w_t \mathbf{T}^T \mathbf{K_t} \mathbf{T} + w_m \mathbf{U}^T \mathbf{K} \mathbf{U}$$

$$\textbf{subject to} \quad V_f(x) \le V_f^* \tag{6}$$
$$\mathbf{K_t}\mathbf{T} = \mathbf{Q_t}$$
$$\mathbf{K}\mathbf{U} = \mathbf{F_m} + \mathbf{F_t}$$

where w_t and w_m determine the relative importance of the heat conduction and structural objectives.

3

D. Level Set Topology Optimization Method

In this work, we employ the level set topology optimization method to generate the training data, which is briefly summarized in this section. More details of the method can be found in [30] and [31].

In the level set topology optimization, the zero level set of an implicit function defines the structural boundary as

$$
\begin{cases}
\phi(\mathbf{x}) \geq 0 & \mathbf{x} \in \Omega \\[2mm]
\phi(\mathbf{x}) = 0 & \mathbf{x} \in \Gamma \\[2mm]
\phi(\mathbf{x}) < 0 & \mathbf{x} \notin \Omega,
\end{cases}
\tag{7}
$$

with ϕ being the level set function, Ω and Γ denoting the structural domain and boundary, respectively. The implicit function is initialized as a signed distance function [32, 33] conventionally.

The optimal boundary is found by solving the following Hamilton-Jacobi equation iteratively

$$
\frac{\partial \phi(\mathbf{x}, t)}{\partial t} + |\nabla \phi(\mathbf{x})| \, V_n(\mathbf{x}) = 0
\tag{8}
$$

where V_n is the normal velocity and t is a fictitious time domain for the level set evolution.

To update the level set function at each node, the following discretized Hamilton-Jacobi equation is solved using an up-wind differential scheme

$$
\phi_r^{k+1} = \phi_r^k - \Delta t \left| \nabla \phi_r^k \right| V_{nr},
\tag{9}
$$

where k is the iteration number, r denotes a discrete node in the design domain, and V_{nr} is the normal velocity at node r. To compute $\left| \nabla \phi_r^k \right|$ for each node, the Hamilton-Jacobi weighted essentially non-oscillatory method (HJ-WENO) is employed. In order to increase the computational efficiency, the level set function is updated only for the nodes that lie within a narrow band around the boundary. This results in ϕ_r having the signed distance property only within the narrow band, and therefore ϕ_r is periodically reinitialized to a signed distance function. The fast-marching method is used for the reinitialization and velocity extension [34].

To obtain the velocities required to update the level set function, the linearized optimization problem

$$
\underset{\Omega}{\textbf{minimize}} \qquad \frac{\partial f}{\partial \Omega^k} \Delta \Omega^k
$$

$$
\tag{10}
$$

$$
\textbf{subject to} \qquad \frac{\partial g_m}{\partial \Omega^k} \Delta \Omega^k \leq -g_m^{-k}
$$

is solved, where f is the objective function, g_m is the mth inequality constraint function, $\Delta \Omega^k$ is the update for the design domain Ω and g_m^{-k} is the change in the mth constraint. Shape derivatives provide information on how the objective and constraint functions change with respect to the boundary movement, and typically take the form of boundary integrals [33]

$$
\frac{\partial f}{\partial \Omega} \Delta \Omega = \Delta t \int_\Gamma s_f V_n d\Gamma
\tag{11}
$$

$$
\frac{\partial g_m}{\partial \Omega} \Delta \Omega = \Delta t \int_\Gamma s_{gm} V_n d\Gamma,
\tag{12}
$$

where s_f and s_{gm} are the shape sensitivity functions for the objective and the mth constraint, respectively. The integrals in Equations 11 and 12 can be estimated as

$$
\frac{\partial f}{\partial \Omega} \Delta \Omega \approx \sum_{j=1}^{nb} \Delta t V_{nj} s_{f,j} l_j = \mathbf{C}_f \cdot \mathbf{V}_n \Delta t
\tag{13}
$$

$$
\frac{\partial g_m}{\partial \Omega} \Delta \Omega \approx \sum_{j=1}^{nb} \Delta t V_{nj} s_{gm,j} l_j = \mathbf{C}_{g_m} \cdot \mathbf{V}_n \Delta t.
\tag{14}
$$

4

In the above expressions, j is a discrete boundary point, V_{nj}, $s_{f,j}$ and $s_{gm,j}$ are the normal velocity and sensitivities at point j for the objective and m^{th} constraint functions, respectively. l_j denotes the length of the local boundary around the boundary point j, $\mathbf{V}_n$ is the vector of normal velocities, and $\mathbf{C}_f$ and $\mathbf{C}_{g_m}$ are vectors containing the product of shape sensitivities and boundary lengths.

For a constrained problem, we have

$$\mathbf{V}_n \Delta t = \alpha \mathbf{d}, \tag{15}$$

where $\mathbf{d}$ is the search direction for the boundary update and $\alpha > 0$ is the distance travelled along the search direction. The optimization problem of Equations 10 and 12 can be reformulated as

$$\underset{\alpha^k, \lambda^k}{\textbf{minimize}} \qquad \Delta t \mathbf{C}_f^k \cdot \mathbf{V}_n^k(\alpha^k, \lambda^k)$$

$$\textbf{subject to} \qquad \Delta t \mathbf{C}_m^k \cdot \mathbf{V}_n^k(\alpha^k, \lambda^k) \le -\bar{\mathbf{g}}_m^k \tag{16}$$

$$\mathbf{V}_{n,\min}^k \le \mathbf{V}_n^k \le \mathbf{V}_{n,\max}^k,$$

with λ denoting Lagrange multipliers for each constraint function. Equation 16 is solved for α^k and λ^k at every iteration k. This method is implemented in the object oriented C++ code [35] and is available as open-source at http://m2do.ucsd.edu/software/. We implemented this method in MATLAB, and use the MATLAB implementation in this work to generate data for the problems that we described in the previous section.

IV. Generative Adversarial Networks

GANs are generative models that learn a mapping from random noise vector z to output image y, $G : z \rightarrow y$ [28]. In GAN, two neural networks contest with each other in a zero-sum game, such that the gain in one network results in loss in the other one. One of these networks is called a generator, which generates new data similar to the original training data. The other network is called the discriminator, which distinguishes whether the data is part of the original data (real) or output of the generator (fake). The loss function in GAN is defined as

$$\mathcal{L}_{GAN}(G, D) = \mathbb{E}_y[\log D(y)] + \mathbb{E}_x[\log(1 - D(G(x)))], \tag{17}$$

where G tries to generate images $G(x)$ that look similar to images from domain Y, while D aims to distinguish between translated samples $G(x)$ and real samples y.

A. Image-to-image Translation GAN

In contrast to GAN, image-to-image conditional GANs learn a mapping from observed image x and random noise vector z, to y, $G : x, z \rightarrow y$. The objective can be expressed as

$$\mathcal{L}_{cGAN}(G, D) = \mathbb{E}_{x,y}[\log D(x, y)] + \mathbb{E}_{x,z}[\log(1 - D(x, G(x, z)))], \tag{18}$$

where G tries to minimize this objective against an adversarial D that tries to maximize it. Previous approaches have combined the GAN objective with a more traditional loss, such as L2 distance [36]. In this work, we employ the method of [37], in which an L1 distance rather than L2 is used, as L1 encourages less blurring:

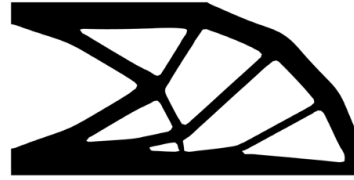$$\mathcal{L}_{L1}(G) = \mathbb{E}_{x,y,z}[\|y - G(x, z)\|_1], \tag{19}$$

The final objective is written as

$$G^* = arg \min_G \max_D \mathcal{L}_{GAN}(G, D) + \lambda \mathcal{L}_{L1}(G). \tag{20}$$

We use this approach to find the mapping between initial strain energy density fields and the optimal topologies.

5
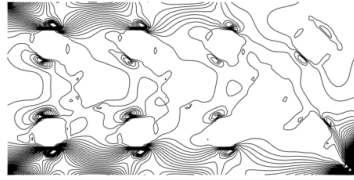
| (a) Strain energy density field | (b) Optimal topology |

Fig. 1 Strain energy density field (left) and optimal topology (right) for a structural problem.

V. Methodology

We are interested in finding a mapping between the boundary conditions and loading and the optimal topologies for multiphysics problems. Adopting the idea of [20], we use the initial structural sensitivity contour plots as the input images. Figure 1 shows an example of a strain energy density contour plot and the corresponding optimal topology. We generate initial strain energy density contour plots and the corresponding optimal topologies for different cases of loading and boundary conditions for structural, heat conduction, and coupled multiphysics problems.

The hypothesis behind this approach is that since optimal topologies in coupled multiphysics problems have a combination of the design features from each of the single-physics solutions, we can learn the solution to a complex multiphysics design problem from the range of relatively straight forward single-physics optimal topologies. To test this hypothesis, we first perform trainings using only single-physics data to find a mapping between strain energy density fields and optimal topologies for structural and heat conduction problems. Then, we perform a training with a combination of single-physics data (structural and heat conduction) to produce concept designs for coupled structural and heat conduction problems. We investigate the effect of adding a small number of multiphysics data to the training data on the predictions. We perform another training with only multiphysics data, and compare the results of these trainings. We use the image-to-image translation GAN described in Section IV.A. The results are presented and discussed in the following section.

VI. Experiments

A. Structural Problems

The first training was performed for structural problems. In this training, we used the strain energy density fields and the corresponding optimal topologies for different cases of loading and boundary conditions. The training data includes 1000 input and 1000 output images, and the test data includes 400 input and 400 output images. Table 1 shows the result of the training for different examples of the test data. The left hand side section shows the strain fields for 25 different cases of loading and boundary conditions. The middle section shows the result of topology optimization for these examples. The trained generator takes in the strain fields and produces the results that are shown in the right hand side section. We can observe that the output of the generator for these inputs cases is very similar to the output of topology optimization for the same cases.

B. Heat Conduction Problems

We performed a similar training for heat conduction problems, in which we used the strain energy density fields and the corresponding optimal topologies for different cases of loading and boundary conditions. The training data includes 1000 input and 1000 output images, and the test data includes 400 input and 400 output images. The results are shown in Table 2. Again, the left hand side section shows the strain fields for 25 different cases of loading and boundary conditions from the test data, the middle section shows the result of topology optimization for these examples and the
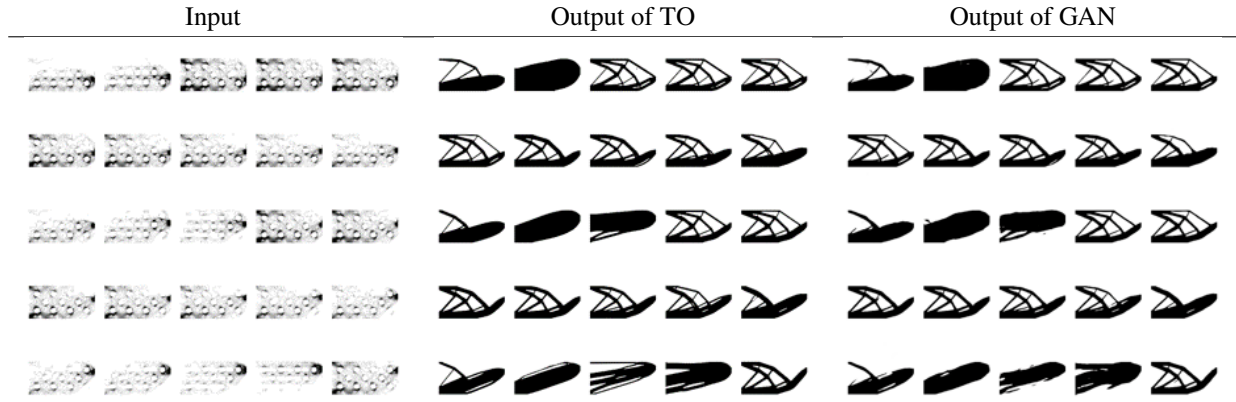
Input	Output of TO	Output of GAN

Table 1   Comparison of optimal topologies from LSTO and the predictions of GAN for structural problems.

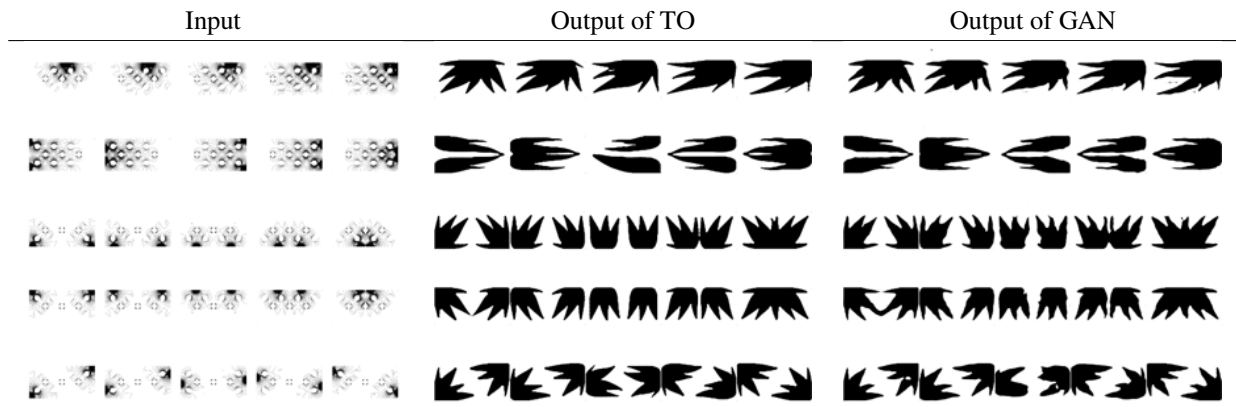| Input	Output of TO	Output of GAN

Table 2   Comparison of optimal topologies from LSTO and the predictions of GAN for heat conduction problems.

right hand side section shows the predictions of the trained generator for the same cases. Similarly, we can observe a high level of visual similarity between the outputs of TO and predictions of GAN.

C. Combining Structural and Heat Conduction Data

Since we are interested in generating concept designs for multiphysics problems, in the next step, we conducted a training step in which the datasets contained both structural and heat conduction data. In this training, we combine 1000 structural and 1000 heat conduction cases. Table 3 shows the results of this training. The left hand side section contains the optimal topologies for 25 different cases of loading and boundary conditions for coupled structural and heat conduction problems. The middle section shows the output of the trained generator for the same cases. As we can see, the outputs of the generator for these multiphysics cases are poor, and do not resemble the output of topology optimization. Furthermore, there are multiple disconnected regions, and the structural integrity is not preserved. This is because the trained model has not seen any multiphysics data at all; therefore, it is not capable of predicting the optimal topologies for the multiphysics problem.

To improve the performance of the generator for the coupled multiphysics problem, we added 400 coupled multiphysics solutions to the training dataset, such that the the training set includes 1000 structural, 1000 heat conduction, and 400 multiphysics data. The results are presented in the right hand side section of Table 3. The predictions of the trained generator for coupled multiphysics problems have improved significantly in comparison with the results of the previous training. In addition to the high level of visual similarity, we can rarely see disconnected regions in these images.

Output of TO	Output of GAN with 1000 structural, 1000 heat conduction and 0 multiphysics data	Output of GAN with 1000 structural, 1000 heat conduction and 400 multiphysics data

Table 3 Comparison of optimal topologies from LSTO and the predictions of GAN for multiphysics problems, using a combined structural and heat conduction training data without (middle) and with (right) multiphyscis data.

D. Different Quantities of Multiphysics Data

Since the generation of coupled multiphysics data is generally more challenging than single-physics data, and we have observed that using a relatively smaller number of multiphysics data can improve the results of training that uses combined single-physics data only, we aim to use the smallest possible number of multiphysics data that gives us satisfactory predictions. Therefore, we perform multiple trainings with different quantities of multiphysics data to observe the effects on the quality of the predictions. We have performed the trainings using 100, 200, 300 and 400 multiphysics data. Tables 4 and 5 show the results of these trainings for 25 and 100 examples, respectively. Each row shows the result of these trainings for a different number of multiphysics data. The left column shows the result of topology optimization for different cases of loading and boundary conditions (the same as those documented in Table 3), and the middle column shows the output of the trained generator for the same cases. We observe that by increasing the amount of multiphysics data, the predictions improve, as expected. We also observe that even using 100 data, the outputs of the generator are clearly better than those in the middle section of Table 3. This means that including multiphysics data with a size equal to only 5% of the size of the single-physics data, can improve the quality of the predictions significantly.

E. Comparison with Trainings Using Only Multiphysics Data

So far, our experiments indicate that by using a combination of single-physics data and a relatively smaller number of multiphysics data, we observe an improvement in the predictions of GAN, in comparison with trainings that did not include any multiphysics data. We have observed that if the number of multiphysics training data is increased, the predictions improve. In this section, we present the results of another set of trainings, in which only multiphysics data is used. We aim to show that the trainings of Section VI.D with combined single-physics and multiphysics data outperform those with only multiphysics data, and therefore using single-physics data can be advantageous in producing concept designs for multiphysics problems. Tables 4 and 5 show the results of these trainings for 25 and 100 examples, respectively. In both tables, the left column includes the results of topology optimization, the middle column includes the predictions of the generator with combined single-physics and multiphysics training data, and the right column includes the predictions of the generator with only multiphysics training data. We observe that, when we use only multiphysics data for training, we have some designs that are completely disconnected, which have no structural integrity. There are also some designs that although connected at a very small region, differ significantly from the output of topology optimization, and contain large regions that are not contributing to load distribution. Two example of these cases are shown in Figure 2. However, we need to use a more quantitative measure of performance to compare these results. We use the objective function as the measure.

Table 6 shows the results of this comparison. To create these plots, we have performed multiple trainings and

8

n	Output of TO	Output of GAN with 1000 structural, 1000 heat conduction and n multiphysics data	Output of GAN with 0 structural, 0 heat conduction and n multiphysics data
100			
200			
300			
400			

Table 4   Comparison of optimal topologies from LSTO and the predictions of GAN for multiphysics problems for trainings with combined single-physics and multiphyscis data (middle), and trainings with only multiphysics data (right), using 100, 200, 300 and 400 multiphysics data.

9

n	Output of TO	Output of GAN with 1000 strutuaral, 1000 heat conduction and n multiphysics data	Output of GAN with 0 strutuaral, 0 heat conduction and n multiphysics data
100			
200			
300			
400			

Table 5   Comparison of optimal topologies from LSTO and the predictions of GAN for multiphysics problems for trainings with combined single-physics and multiphyscis data (middle), and trainings with only multiphysics data (right), using 100, 200, 300 and 400 multiphysics data.

Fig. 2   Examples of predictions of the generator trained with only multiphysics data that are completely disconnected and result in very large values of the objective function.

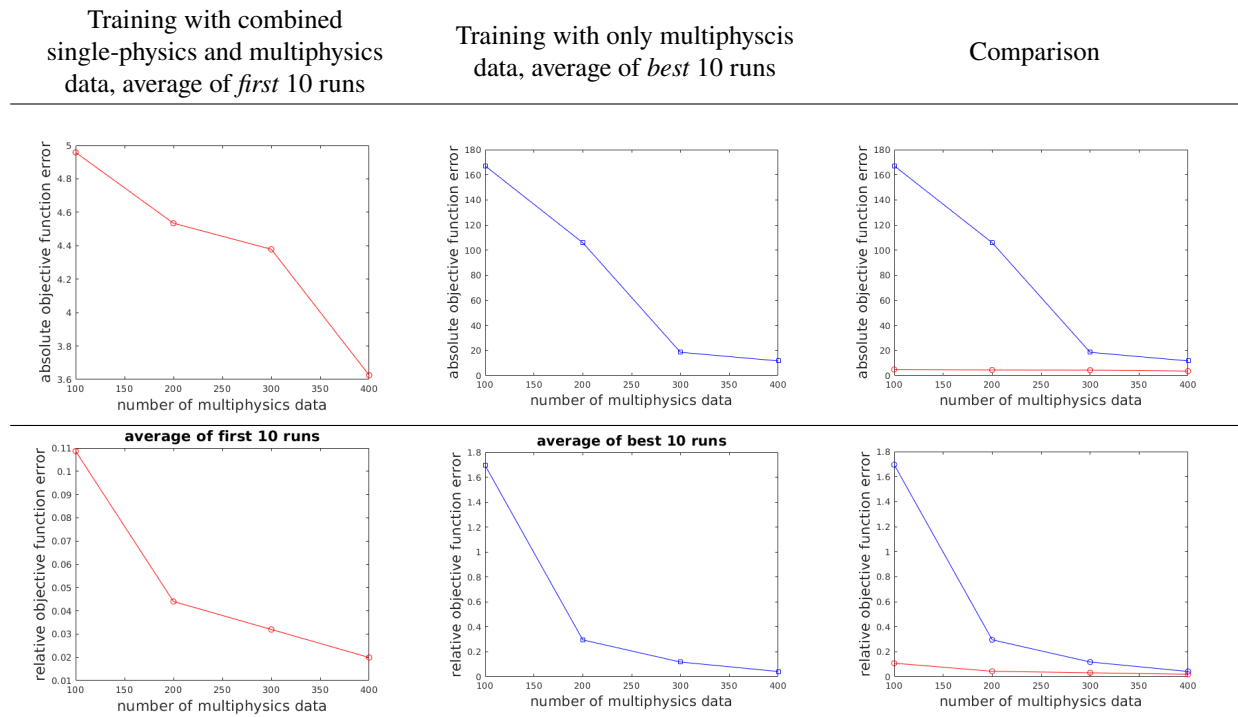| Training with combined single-physics and multiphysics data, average of *first* 10 runs	Training with only multiphyscis data, average of *best* 10 runs	Comparison

Table 6   Comparison of the objective function difference between the outputs of the trained generator and the optimal topologies produced by LSTO, for trainings with combined multiphysics and single-physics data (left), and the trainings with only multiphysics data (middle). The first row includes the plots with the absolute objective function error, and the second row includes the plots with relative objective function error.

11

computed the average objective function errors of all trainings. For trainings with combined single-physics and multiphysics data, we repeated the trainings 10 times. For trainings with only multiphysics data, we repeated the trainings more, since in some cases the error was orders of magnitude larger, due to the existence of some designs that were completely disconnected (cf. Figure 2). Therefore, for trainings with combined single-physics and multiphysics data, we use the *first* 10 trainings and for trainings with only multiphysics data, we use the *best* 10 trainings to avoid those cases. The top and bottom rows of the table indicate the absolute and relative objective function error plots, respectively. The plots in the left column show the error as a function of the number of multiphysics data for trainings with combined single-physics and multiphysics data (Section VI.D). The plots in the middle column show the errors as a function of the number of multiphysics data for trainings with only multiphysics data. On the right hand side, we can see the comparison between these trainings. We observe that using single-physics data in combination of multiphysics data decreases the objective function error by two orders of magnitude.

VII. Conclusions

In this work, we presented a method for designing concepts for multiphysics problems using GANs. We used an image-to-image translation GAN algorithm to find a mapping between the strain energy density fields and the optimal topologies for structural and heat conduction problems, and we observed high visual resemblance between the ground truth generated by level-set topology optimization and output of GANs. We performed trainings with a combination of structural and heat conduction data, with and without multiphysics data. We observed that with no multiphysics data in the training dataset, the generator was unable to generate meaningful concepts for multiphysics problems. However, adding a relatively small number of multiphysics data improved the results significantly. We performed this training using different numbers of multiphysics data and observed that increasing the number of multiphysics data improved the results, as expected. We also performed trainings using only multiphysics data. We computed the average objective function error for trainings with combined single-physics and multiphysics data, and trainings with only multiphysics data. The results demonstrated that using single-physics data is beneficial in designing concepts for coupled multiphysics problems.

Acknowledgment

References

[1] Bendsøe, M. P., and Kikuchi, N., "Generating optimal topologies in structural design using a homogenization method," *Computer methods in applied mechanics and engineering*, Vol. 71, No. 2, 1988, pp. 197–224.

[2] Suzuki, K., and Kikuchi, N., "A homogenization method for shape and topology optimization," *Computer methods in applied mechanics and engineering*, Vol. 93, No. 3, 1991, pp. 291–318.

[3] Bendsøe, M. P., and Sigmund, O., "Material interpolation schemes in topology optimization," *Archive of applied mechanics*, Vol. 69, No. 9, 1999, pp. 635–654.

[4] Sigmund, O., "Morphology-based black and white filters for topology optimization," *Structural and Multidisciplinary Optimization*, Vol. 33, No. 4-5, 2007, pp. 401–424.

[5] Norato, J., Bell, B., and Tortorelli, D. A., "A geometry projection method for continuum-based topology optimization with discrete elements," *Computer Methods in Applied Mechanics and Engineering*, Vol. 293, 2015, pp. 306–327.

[6] Kazemi, H., Vaziri, A., and Norato, J. A., "Topology optimization of structures made of discrete geometric components with different materials," *Journal of Mechanical Design*, Vol. 140, No. 11, 2018, p. 111401.

[7] Kazemi, H., Vaziri, A., and Norato, J., "Topology optimization of multi-material lattices for maximal bulk modulus," *International Design Engineering Technical Conferences and Computers and Information in Engineering Conference*, Vol. 59186, American Society of Mechanical Engineers, 2019, p. V02AT03A052.

[8] Kazemi, H., Vaziri, A., and Norato, J. A., "Multi-material topology optimization of lattice structures using geometry projection," *Computer Methods in Applied Mechanics and Engineering*, Vol. 363, 2020, p. 112895.

[9] Kazemi, H., and Norato, J. A., "Topology optimization of lattices with anisotropic struts," *Structural and Multidisciplinary Optimization*, Vol. 63, No. 4, 2021, pp. 1653–1668.

[10] Allaire, G., Jouve, F., and Toader, A.-M., "A level-set method for shape optimization," *Comptes Rendus Mathematique*, Vol. 334, No. 12, 2002, pp. 1125–1130.

[11] Allaire, G., Jouve, F., and Toader, A.-M., "Structural optimization using sensitivity analysis and a level-set method," *Journal of computational physics*, Vol. 194, No. 1, 2004, pp. 363–393.

[12] Allaire, G., De Gournay, F., Jouve, F., and Toader, A.-M., "Structural optimization using topological and shape sensitivity via a level set method," *Control and cybernetics*, Vol. 34, No. 1, 2005, p. 59.

[13] Dunning, P. D., and Kim, H. A., "Introducing the sequential linear programming level-set method for topology optimization," *Structural and Multidisciplinary Optimization*, Vol. 51, No. 3, 2015, pp. 631–643.

[14] Dunning, P. D., Kim, H. A., and Mullineux, G., "Investigation and improvement of sensitivity computation using the area-fraction weighted fixed grid FEM and structural optimization," *Finite Elements in Analysis and Design*, Vol. 47, No. 8, 2011, pp. 933–941.

[15] Hoyer, S., Sohl-Dickstein, J., and Greydanus, S., "Neural reparameterization improves structural optimization," *arXiv preprint arXiv:1909.04240*, 2019.

[16] Zhang, Y., Peng, B., Zhou, X., Xiang, C., and Wang, D., "A deep convolutional neural network for topology optimization with strong generalization ability," *arXiv preprint arXiv:1901.07761*, 2019.

[17] Cang, R., Yao, H., and Ren, Y., "One-shot generation of near-optimal topology through theory-driven machine learning," *Computer-Aided Design*, Vol. 109, 2019, pp. 12–21.

[18] Yu, Y., Hur, T., Jung, J., and Jang, I. G., "Deep learning for determining a near-optimal topological design without any iteration," *Structural and Multidisciplinary Optimization*, Vol. 59, No. 3, 2019, pp. 787–799.

[19] Chandrasekhar, A., and Suresh, K., "TOuNN: Topology optimization using neural networks," *Structural and Multidisciplinary Optimization*, Vol. 63, No. 3, 2021, pp. 1135–1149.

[20] Nie, Z., Lin, T., Jiang, H., and Kara, L. B., "Topologygan: Topology optimization using generative adversarial networks based on physical fields over the initial domain," *Journal of Mechanical Design*, Vol. 143, No. 3, 2021, p. 031715.

[21] Kallioras, N. A., Kazakis, G., and Lagaros, N. D., "Accelerated topology optimization by means of deep learning," *Structural and Multidisciplinary Optimization*, Vol. 62, No. 3, 2020, pp. 1185–1212.

[22] Lin, Q., Hong, J., Liu, Z., Li, B., and Wang, J., "Investigation into the topology optimization for conductive heat transfer based on deep learning approach," *International Communications in Heat and Mass Transfer*, Vol. 97, 2018, pp. 103–109.

[23] Li, B., Huang, C., Li, X., Zheng, S., and Hong, J., "Non-iterative structural topology optimization using deep learning," *Computer-Aided Design*, Vol. 115, 2019, pp. 172–180.

[24] Li, B., Tang, W., Ding, S., and Hong, J., "A generative design method for structural topology optimization via transformable triangular mesh (TTM) algorithm," *Structural and multidisciplinary optimization*, Vol. 62, No. 3, 2020, pp. 1159–1183.

[25] Guo, T., Lohan, D. J., Cang, R., Ren, M. Y., and Allison, J. T., "An indirect design representation for topology optimization using variational autoencoder and style transfer," *2018 AIAA/ASCE/AHS/ASC Structures, Structural Dynamics, and Materials Conference*, 2018, p. 0804.

[26] Oh, S., Jung, Y., Kim, S., Lee, I., and Kang, N., "Deep generative design: Integration of topology optimization and generative models," *Journal of Mechanical Design*, Vol. 141, No. 11, 2019.

[27] Sharpe, C., and Seepersad, C. C., "Topology design with conditional generative adversarial networks," *International Design Engineering Technical Conferences and Computers and Information in Engineering Conference*, Vol. 59186, American Society of Mechanical Engineers, 2019, p. V02AT03A062.

[28] Goodfellow, I. J., Pouget-Abadie, J., Mirza, M., Xu, B., Warde-Farley, D., Ozair, S., Courville, A., and Bengio, Y., "Generative adversarial networks," *arXiv preprint arXiv:1406.2661*, 2014.

13

[29] Eslami, M. R., Hetnarski, R. B., Ignaczak, J., Noda, N., Sumi, N., and Tanigawa, Y., *Theory of elasticity and thermal stresses*, Vol. 197, Springer, 2013.

[30] Hedges, L. O., Kim, H. A., and Jack, R. L., "Stochastic level-set method for shape optimisation." *Journal of Computational Physics*, Vol. 348, 2017, pp. 82–107.

[31] Picelli, R., Townsend, S., Brampton, C., Norato, J., and Kim, H., "Stress-based shape and topology optimization with the level set method," *Computer Methods in Applied Mechanics and Engineering*, Vol. 329, 2018, pp. 1–23.

[32] Wang, M. Y., Wang, X., and Guo, D., "A level set method for structural topology optimization," *Computer Methods in Applied Mechanics and Engineering*, Vol. 192, 2003, pp. 227–246.

[33] Allaire, G., Jouve, F., and Toader, A. M., "Structural optimization using sensitivity analysis and a level-set method," *Journal of Computational Physics*, Vol. 194, 2004, pp. 363–393.

[34] Sethian, J., "A fast marching level set method for monotonically advancing fronts," *Proceedings of the National Academy of Sciences*, Vol. 93, No. 4, 1996, pp. 1591–1595.

[35] Sandilya, K., Du, Z., Chung, H., Kim, H. A., Jauregui, C., Townsend, S., Picelli, R., Zhou, X. Y., and Hedges, L., "OpenLSTO: Open-Source Software for Level Set Topology Optimization," *Multidisciplinary Analysis and Optimization Conference*, 2018, p. 3882.

[36] Pathak, D., Krahenbuhl, P., Donahue, J., Darrell, T., and Efros, A. A., "Context encoders: Feature learning by inpainting," *Proceedings of the IEEE conference on computer vision and pattern recognition*, 2016, pp. 2536–2544.

[37] Isola, P., Zhu, J.-Y., Zhou, T., and Efros, A. A., "Image-to-image translation with conditional adversarial networks," *Proceedings of the IEEE conference on computer vision and pattern recognition*, 2017, pp. 1125–1134.